Tetrahedron: *Asymmetry* 20 (2009) 1759–1766

Contents lists available at ScienceDirect

Tetrahedron: *Asymmetry*

journal homepage: www.elsevier.com/locate/tetasy

The synthesis and conformational analysis of optical isomers of 4-phenyl-perhydropyrido[1,2-*a*]pyrazine-1,3-dione: an example of 'solid state–frozen' dynamics in nitrogen-bridged bicyclic 2,6-diketopiperazines

Maciej Dawidowski [a,*], Franciszek Herold [a], Marcin Wilczek [b], Jerzy Kleps [a], Irena Wolska [c], Jadwiga Turło [a], Andrzej Chodkowski [a], Paweł Widomski [d], Anna Bielejewska [d]

[a] *Department of Drug Technology, Faculty of Pharmacy, Medical University of Warsaw, Banacha 1 Str., 02-097 Warszawa, Poland*
[b] *Laboratory of NMR Spectroscopy, Faculty of Chemistry, University of Warsaw, Pasteura 1 Str., 02-093 Warszawa, Poland*
[c] *Department of Crystallography, Faculty of Chemistry, Adam Mickiewicz University, Grunwaldzka 6 Str., 60-780 Poznań, Poland*
[d] *Institute of Physical Chemistry, Polish Academy of Sciences, Kasprzaka 44/52 Str., 02-224 Warszawa, Poland*

ARTICLE INFO

Article history:
Received 18 May 2009
Accepted 26 June 2009
Available online 10 August 2009

ABSTRACT

The synthesis, chemical properties, and conformational analysis of enantiopure (4*R*,9a*S*)-, (4*S*,9a*R*)-, (4*S*,9a*S*)-, and (4*R*,9a*R*)-4-phenyl-perhydropyrido[1,2-*a*]pyrazine-1,3-diones having potential biological activity are described. An interesting example of the coexistence of two invertomers of the (4*R*,9a*R*)-diastereomer in a single crystal unit cell is reported. The invertomers differ in the *cis*/*trans*-relationship between the fused rings and in the absolute configuration at the chiral nitrogen atom. The structure and equilibrium distributions of the respective conformers have been determined by NMR spectroscopy in both polar and non-polar solvents at various temperatures. The NMR spectra show that dynamic processes in the imide parts of the interconverting species are restrained by self-aggregation. The (4*S*,9a*R*)-diastereomer exists in a single conformation with insignificant dynamic effects.

1. Introduction

Cyclic imides are widely recognized as valuable components of biologically active molecules. Among the most important of these agents are anticonvulsants,[1] antiangiogenic agents,[2] and the compounds that affect serotonin (5-HT) neurotransmission.[3] The imide moiety is also present in various pharmacologically active natural products.

Over the last few decades, much attention has been paid to 2,5-diketopiperazines (2,5-DKPs) as useful scaffolds for the development of pharmacologically active agents. The group of their constitutional isomers bearing the imide moiety—2,6-diketopiperazines (2,6-DKPs), has been slightly less explored. DKPs are known to possess various pharmaceutical activities, such as antitumor, anticonvulsant, and antiviral. Their usefulness for medicinal chemists is greatly increased by several factors, such as the ability to mimic peptidic pharmacophores, resistance to proteolytic enzymes, conformational rigidity, and the capability of forming hydrogen bonds. Frequently, these small heterocyclic systems are derived from amino acids, and in most cases, enantiopure compounds are easily accessible through relatively simple synthetic procedures. Moreover, DKPs can also be obtained using combinatorial chemistry, which allows the creation of libraries of chiral compounds for biological screening and structure-activity relationship (SAR) studies.[4]

Recently, we described a convenient route to proline-derived bicyclic 2,6-DKP scaffolds with base-promoted intramolecular cyclocondensation as a key step.[5] The ongoing medicinal chemistry project required the synthesis of the six-membered homologues of the above compounds in enantiopure forms. It was also of our interest to determine the features that can contribute to SAR analysis, such as crystal structure, structure and flexibility in solution, and hydrogen-bonding capability of the compounds obtained, with particular focus on differentiating each respective diastereomeric pair. As nitrogen-bridged bicyclic compounds are known to undergo complex dynamic processes due to N-inversion,[6] the conformational features of the molecules synthesized were characterized by variable-temperature NMR measurements. An interesting example of inversion on the chiral nitrogen that is 'frozen' in the solid state is presented in the form of XRD data.

2. Results and discussion

2.1. Synthesis

Only the synthetic pathways to (4*R*,9a*S*)-**4** and (4*S*,9a*S*)-**6** are presented for clarity. The same route from (*R*)-(+)-2-piperidinecarboxylic acid (*R*)-**1** was chosen for the antipodes (4*S*,9a*R*)-**4** and

* Corresponding author. Tel.: +48 22 5720646; fax: +48 22 5720647.
E-mail address: maciej.dawidowski@wum.edu.pl (M. Dawidowski).

0957-4166/$ - see front matter © 2009 Elsevier Ltd. All rights reserved.
doi:10.1016/j.tetasy.2009.06.022

(4*R*,9a*R*)-**6** with equal results. The characterization details are provided in Section 4.

The target compounds (4*R*,9a*S*)-4-phenyl-perhydropyrido[1,2-*a*]pyrazine-1,3-dione (4*R*,9a*S*)-4, and (4*S*,9a*S*)-4-phenyl-perhydropyrido[1,2-*a*]pyrazine-1,3-dione (4*S*,9a*S*)-6, were synthesized by the intramolecular cyclocondensation of the corresponding (2*S*,α*R*)- and (2*S*,α*S*)-α-(2-carbamoylpiperidinyl)-α-phenylacetic acid methyl esters (2*S*,α*R*)-3 and (2*S*,α*S*)-5, as outlined in Scheme 1.

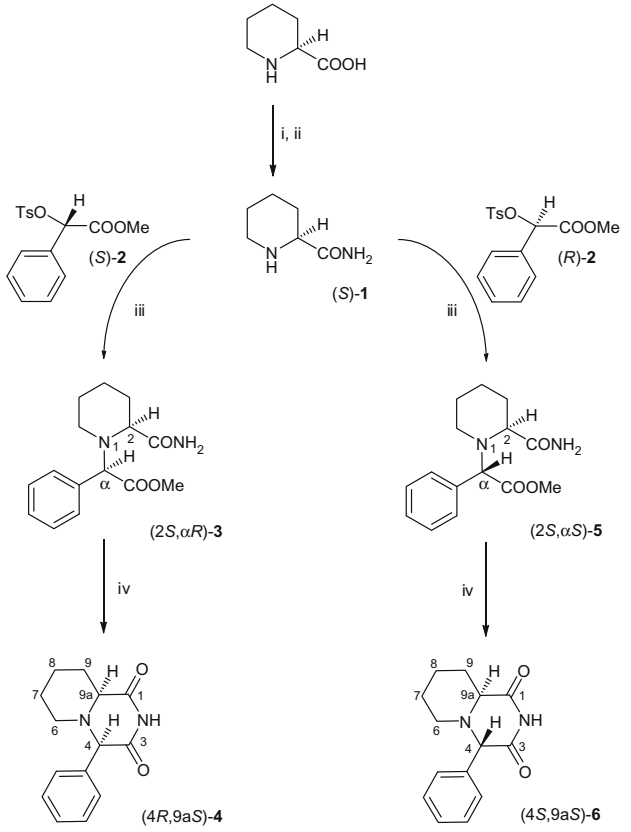

Scheme 1. Reagents and conditions: (i) $SOCl_2$ (1.0 equiv), MeOH, reflux, 2 h; (ii) $NH_{3\ (g)}$, MeOH, rt, 48 h; (iii) MeCN, pyridine (1.0 equiv), reflux, 1 h; (iv) NaOH (1.0 equiv), EtOH, rt, 15 min.

Enantiopure (*S*)-(−)-2-piperidinecarboxylic acid was used as a substrate for the synthesis. The esterification of the amino acid, followed by ammonolysis of the resulting ester yielded enantiomerically pure (*S*)-(−)-2-piperidinecarboxamide (*S*)-**1**. (*S*)-(+)- and (*R*)-(+)-2-(4-toluenesulfonyloxy)-phenylacetic acid methyl esters (*S*)-**2** and (*R*)-**2**, respectively, required for the synthesis were obtained by well-established methods.[5,7]

It appeared convenient to directly obtain the target cyclic imides **4** and **6** without isolating the intermediate amidoesters **3** and **5**. Therefore, one-pot N-alkylation of pipecolinamide (*S*)-**1** with tosylates **2**, and the subsequent cyclocondensation using an excess of potassium carbonate in rigorously dried acetonitrile were investigated. The reaction was found to proceed with epimerization at the C-4 stereocenter of the final product, leading to the mixtures of (4*R*,9a*S*)-**4** and (4*S*,9a*S*)-**6**. Compound (4*R*,9a*S*)-**4** was found to be the major product, regardless of whether (*S*)-**2**, (*R*)-**2**, or *rac*-**2** was used as the starting material (Table 1). The epimerization can be easily explained by the fact that the relatively acidic H-4 protons of (4*R*,9a*S*)-**4** and (4*S*,9a*S*)-**6** are prone to enolization under prolonged exposure to basic conditions. The experiment, consisting of refluxing pure (4*R*,9a*S*)-**4** and (4*S*,9a*S*)-**6**, in CD_3CN in the presence

Table 1
One-pot N-alkylation of (*S*)-pipecolinamide and cyclocondensation to imides **4** and **6**

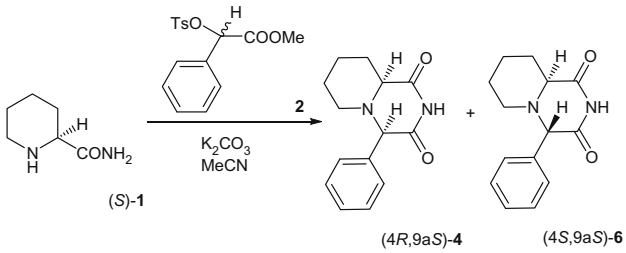

Entry	Alkylating agent	Conditions[a]	dr[b]	Yield[c] (%)
1	*rac*-**2**	2.0 equiv K_2CO_3, 2.5 h	76/24	65
2	(*S*)-**2**		70/30	52
3	(*R*)-**2**		81/19	nd
4	(*R*)-**2**	1.5 equiv K_2CO_3, 1.5 h	67/33	35
5	(*R*)-**2**	1.0 equiv K_2CO_3, TBAB, 8 h	54/46	30

nd—not determined.
[a] For each entry the reaction was carried out in refluxing MeCN.
[b] dr of (4*R*,9a*S*)-**4**/(4*S*,9a*S*)-**6**.
[c] Isolated yield.

of potassium carbonate (1.0 equiv) and D_2O (trace), led to the formation of 7:3 equilibrium mixtures of (4*R*,9a*S*)-**4**/(4*S*,9a*S*)-**6** in both cases. Under these conditions, proton–deuterium exchange was observed, with the complete disappearance of H-4 resonances from the ^1H NMR spectrum. The two H-9a signals corresponding to the respective diastereomers remained unchanged, indicating that no epimerization occurred at the C-9a stereocenter. Although no enantiomeric mixtures were formed, the obtained mixture of (4*R*,9a*S*)-**4** and (4*S*,9a*S*)-**6** could not be efficiently separated on the required (>1.5 mmol) scale.[†] Moreover, the overall chemical yield was significantly diminished, most probably due to the base-induced partial decomposition of the starting tosylate **2**.

To obtain target compounds of high enantiomeric purity, the two-step route involving (1) the synthesis and isolation, and (2) the subsequent cyclocondensation of the respective amidoesters (2*S*,α*R*)-**3** and (2*S*,α*S*)-**5** was pursued (Scheme 1). In all cases, enantiopure (*S*)-**1** and (*S*)-**2** or (*R*)-**2** were used as the starting materials. The results are summarized in Tables 2 and 3.

For the N-alkylation step, a polar aprotic solvent was chosen because it proved to ensure both the good solubility of the reactants and excellent conversions even at room temperature. Considering that the use of a strong base would most probably cause unwanted side reactions, thus lowering both the enantiomeric purity and yield of **3** (Table 2 and Ref. 5), a weak organic base was investigated. Triethylamine was found to diminish the enantiomeric purity of the starting tosylate **2** under both prolonged and short times of exposure. Pyridine was found to be more convenient for the N-alkylation step, as it promoted neither the significant epimerization of the base-sensitive tosylate nor the cyclocondensation of the alkylation products **3**. The (2*S*,α*S*)-**5** isomer was obtained in a higher diastereomeric ratio (dr = 99/1) than (2*S*,α*R*)-**3** (dr = 90/10) in analogous reactions, as estimated by HPLC of the crude post-reaction mixtures. The analytically pure samples of (2*S*,α*R*)-**3** and (2*S*,α*S*)-**5** were obtained using fractional recrystallization from a non-polar solvent system.

Notably, the diastereomeric ratio (dr = 73/27) of the N-alkylation of (*S*)-(−)-pipecolinamide with racemic (*R*,*S*)-2-(4-toluene-

[†] Separation by column chromatography failed due to two reasons: very similar R_f values (TLC: ΔR_f <0.1) of the products and their poor solubility in the non-polar solvent systems required for at least partial separation. Fractional recrystallization of the mixture from lower alcohols was found to be only partially effective due to the similar solubility of both diastereoisomers in the recrystallization solvents.

Table 2
N-Alkylation of (*S*)-**1** and L-prolineamide with 2-(4-toluenesulfonyloxy)-phenylacetic acid methyl esters

Entry	Substrate	Alkylating agent	Conditions[a]	dr[b]	Yield[e] (%)
1	L-Prolineamide	*rac*-**2**	Et_3N, MeCN, rt, 48 h	43/57[c]	88
2	(*S*)-**1**	*rac*-**2**		27/73[d]	92
3	(*S*)-**1**	(*S*)-**2** or (*R*)-**2**		27/73	nd
4	(*S*)-**1**	*rac*-**2**	Pyridine, MeCN, rt, 48 h	30/70	95
5	(*S*)-**1**	(*S*)-**2**	Et_3N, MeCN, reflux, 1 h	43/57	nd
6	(*S*)-**1**	(*R*)-**2**		14/86	nd
7	(*S*)-**1**	(*S*)-**2**	Pyridine, MeCN, reflux, 1 h	90/10	84
8	(*S*)-**1**	(*R*)-**2**		1/99	90
9	(*S*)-**1**	*rac*-**2**	Pyridine, $PhCH_3$, reflux, 1.5 h	30/70	63

nd—not determined.
[a] For each entry 1.1 equiv of base was used.
[b] dr of (2*S*,α*R*)-**3**/(2*S*,α*S*)-**5** estimated by HPLC of the crude products.
[c] dr of (2*S*,α*R*)-/(2*S*,α*S*)-isomer, as in Ref. 5.
[d] Estimated by GC/MS of the crude post-reaction mixture.
[e] Isolated yield.

Table 3
NaOH-catalyzed cyclocondensation of (2*S*,α*R*)-**3** and (2*S*,α*S*)-**5**

Entry	Substrate	dr[a]	er[b]	Yield[c] (%)
1	(2*S*,α*R*)-**3**	91/9	>99/1	92
2	(2*S*,α*S*)-**5**	3/97	>99/1	94

[a] dr of (4*R*,9a*S*)-**4**/(4*S*,9a*S*)-**6**.
[b] Estimated by chiral HPLC analysis of the crude products.
[c] Isolated yield.

sulfonyloxy)-phenylacetic acid methyl ester *rac*-**2** under mild conditions was about threefold higher compared to the analogous reaction for its homologue, L-prolineamide (dr = 57/43, refer Table 1 and Ref. 5). The sense of diastereoinduction in both cases was the same and it favored the (*S*,*S*) products. This suggests that the mechanism of this partial stereoselectivity is similar in both cases and could be due to the geometric differences between a five-membered ring and a six-membered ring. All attempts toward diastereomeric resolution from this mixture, either by column chromatography or by fractional crystallization, failed.

Compounds (2*S*,α*R*)-**3** and (2*S*,α*S*)-**5** obtained from enantiopure (*S*)-**1** and (*S*)-**2** or (*R*)-**2**, respectively, were then converted to the corresponding cyclic imides (4*R*,9a*S*)-**4** and (4*S*,9a*S*)-**6** through base-catalyzed intramolecular cycloaddition in a polar protic solvent (EtOH). Since cyclocondensation catalyzed by weak bases in heterogeneous system is slow, requires heating, and consequently results in significant epimerization of the products, the reaction was hastened by using a strong base under homogenous conditions (see also Ref. 5). The reaction proceeded rapidly with 1.0 equiv of NaOH and was followed by immediate quenching and standard work-up, yielding almost pure stereoisomers, as estimated by chiral HPLC analysis of the crude products. Notably, the cyclocondensation of (2*S*,α*R*)-**3** was accompanied by a slightly higher degree of epimerization at C-4 than in the case of (2*S*,α*S*)-**5**. Analytical samples of the target compounds were then prepared by a single recrystallization from absolute ethanol.

2.2. Structural investigations

At room temperature, each of the multiplets in the aliphatic region of the ^{1}H NMR spectrum of (4*S*,9a*R*)-**4** in $CDCl_3$ was a sharp signal, which enabled the accurate estimation of the geminal and vicinal coupling constants.

The multiplet of H-9a proton at annelation (doublet of doublets) was found to be particularly helpful in conformational analysis. The two vicinal coupling constants, $^3J_{9a\text{-}9ax}$ = 11.2 Hz and $^3J_{9a\text{-}9eq}$ = 2.8 Hz, corresponded to the dihedral angles of ~180° and ~50° (estimated according to the Karplus equation[8]), and indicated the *axial*-position of H-9a with respect to the piperidine framework, with the H-C9a bond situated outside the H-9$_{ax}$–C9–H-9$_{eq}$ plane.

The relative stereochemistry of (4*S*,9a*R*)-**4** was ascertained by the strong mutual NOE effects between H-4 and H-9a. Other interactions were observed between H-4 and H-6$_{ax}$, H-6$_{eq}$, aromatic protons and between H-9a and H-9$_{eq}$, H-8$_{ax}$, H-6$_{ax}$.

Considering the above results, at room temperature, the solution structure of (4*S*,9a*R*)-**4** is consistent with the model generated by theoretical calculations (Fig. 1) and it indicates a persistence of the *trans*-chair/sofa conformation exclusively. Most probably, ring inversion is disfavored due to steric reasons. Moreover, it also appears that the piperidine framework is particularly rigid; thus, interconversion cannot be observed in the temperature range of −60 to 50 °C ($CDCl_3$) used for the NMR experiments.

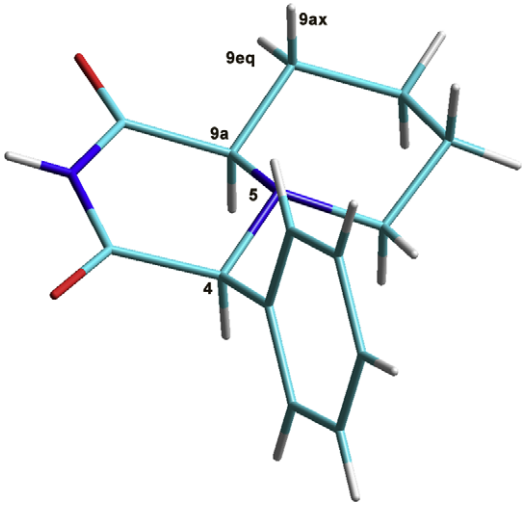

Figure 1. The optimized structure of (4*S*,9a*R*)-**4**, together with the numbering of atoms essential for the conformational analysis. The analysis of torsion angles indicates the *trans*-chair/sofa conformation of the fused piperidine and piperazine-1,3-dione rings. The arrangement of the hydrogen H-4 and the nitrogen N-5 lone pair is *trans*-diaxial, with respect to the piperazine framework. The chiral N-5 atom adopts the (*S*)-configuration.

According to the XRD measurements, (4*R*,9a*R*)-**6** crystallizes in the monoclinic $P2_1$ space group with two distinct invertomers **A** and **B** in the asymmetric unit cell. These conformers are joined through N2A–H2A···O1B (−*x*, *y* + 1/2, −*z* + 1) and N2B–H2B···O1A (−*x*, *y* − 1/2, −*z* + 1) links, forming **AB** dimers (Figs. 2 and 3, Table 4).

The conformation of **A** can be described as a *cis*-chair/sofa with a *cis-axial/equatorial* arrangement of the nitrogen N-5 lone pair and

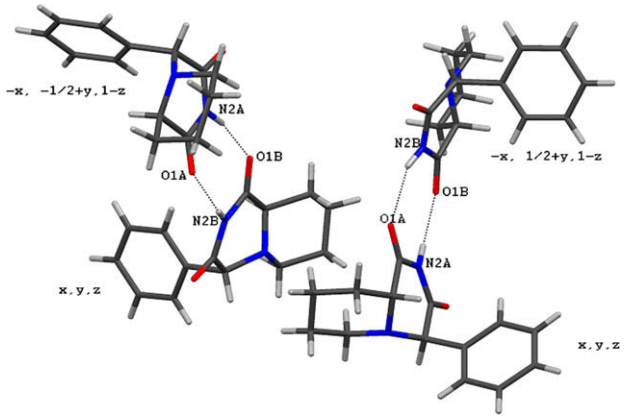

Figure 2. The **AB** dimers of (4*R*,9a*R*)-**6**.

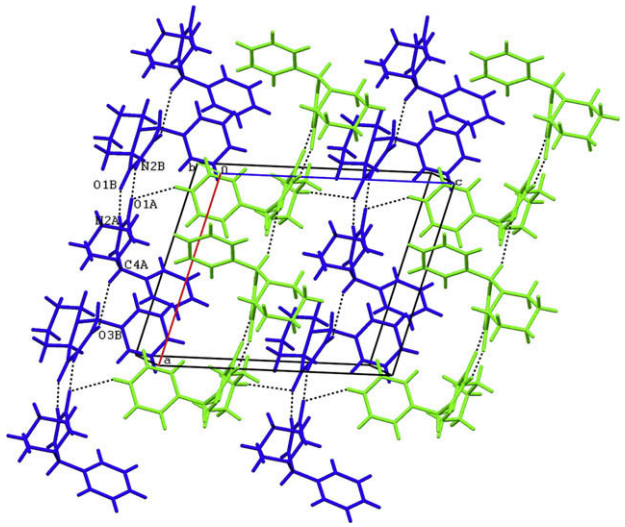

Figure 3. Projection of the crystal structure of (4*R*,9a*R*)-**6**. The **AB** dimers are linked by C4A–H4A···O3B($-x+1$, $y+1/2$, $-z+1$) interactions to form chains parallel to the *a*-axis (blue and green color). The other contacts (refer Table 4) join the chains to create a three-dimensional network.

Table 4
Hydrogen-bonding geometry for (4*R*,9a*R*)-**6** (Å and °)

D–H···A	*d*(D–H)	*d*(H···A)	*d*(D···A)	<(DHA)
*Compound (4R,9aR)-**6***				
N2A–H2A···O1B^{i}	0.86	2.07	2.922(1)	169
N2B–H2B···O1A^{ii}	0.86	2.26	3.073(2)	159
C8B–H8BA···O1B^{i}	0.97	2.69	3.572(2)	151
C4A–H4A···O3B^{iii}	0.98	2.66	3.565(2)	153
C4'B–H4'B···O1A^{iv}	0.93	2.58	3.420(2)	150
C8B–H8BB···O3B^{v}	0.97	2.71	3.305(2)	120
C7B–H7BA···O3B^{v}	0.97	2.63	3.318(2)	128

Symmetry codes: (i) $-x, y+1/2, -z+1$; (ii) $-x, y-1/2, -z+1$; (iii) $-x+1, y+1/2, -z+1$; (iv) $x, y, z-1$; (v) $x, y+1, z$.

the hydrogen at annelation (H-9a), with respect to the piperidine ring.

Molecule **B** adopts the trans-chair/sofa conformation with a *trans*-diaxial arrangement of the nitrogen N-5 lone pair and the hydrogen at annelation (H-9a).

For the respective conformers, the absolute configuration on the chiral nitrogen atom at the annelation (N-5) is different and can be assigned as follows: (*R*)- for **A** and (*S*)- for **B**.

The aliphatic region of the ^{1}H NMR spectrum of (4*R*,9a*R*)-**6** recorded in $CDCl_3$ at room temperature was composed of broadened and overlapped signals, which indicated that the ^{1}H NMR spectrum of (4*R*,9a*R*)-**6** was largely affected by dynamic processes. Indeed, in acetone-d_6 the coalescence of most peaks took place at about −41 °C, followed by the development of two sets of signals in a ratio of 1.3:1 (Fig. 4). The low-temperature 2D (^{1}H–^{1}H COSY; HSQC) experiments, the analysis of the integral values and the chemical shifts of each signal established the peak assignments shown in Table 5.

The H-6$_{ax}$ proton of **B** lay in the relatively high-field region of the spectrum, whereas the corresponding signal in the **A** conformer was significantly shifted toward the lower field ($\Delta\delta_{A-B}$ = 0.75 ppm, acetone-d_6). The remarkable high-field shift of H-6$_{ax}$ can be attributed to the anisotropic effect of the phenyl ring present in the spatial vicinity of the **B** conformer. On the contrary, no such effect can be considered in **A** due to the large distance between H-6$_{ax}$ and the phenyl moiety.

The intensities of the low-temperature ^{1}H–^{1}H COSY cross-peaks H-9a/H-9$_{ax}$ and H-9a/H-9$_{eq}$ in the **B** conformer differed, which could be attributed to the unequal couplings of H-9a with neighboring protons. This suggested that the H-C9a bond was situated outside the H-9$_{ax}$–C9–H-9$_{eq}$ plane. On the contrary, the corresponding cross-peaks in **A** were of similar intensities, thus the H-C9a bond was located inside the above-mentioned plane.

The populations of the two conformers determined from the ^{1}H NMR spectra in acetone-d_6 corresponded to a very small free-energy difference of 0.5 kJ/mol at −41 °C, as calculated using the Eyring equation for the H-4 proton.[9] Energy optimization with the AM1 semiempirical method showed that the gas-phase conformations were essentially isoenergetic, with an energy difference of 0.1 kJ/mol favoring the **B** invertomer. Slightly different equilibrium distributions were elucidated from the ^{1}H NMR spectra in other solvents. Thus, the **B**/**A** ratio was 1:1.3 in $CDCl_3$ and 1.5:1 in CD_3OD. In general, in the solvent with a more polar nature, the *trans*-sofa/chair conformation appears to be increasingly favored. If the above conclusion can be at least roughly extrapolated to biological systems mostly containing water, this feature can be of importance for correlating the biological activity of a molecule with its structure.

A careful study of the ^{1}H and ^{13}C NMR temperature spectra in $CDCl_3$ showed an unusual feature. Below the coalescence, two sets of signals of the H-2 protons and the C-1 and C-3 carbons of the imide moiety were visible in the NMR spectra. Notably, when the sample was warmed to room temperature, the imide-NH peaks remained split at the same ratio for a short period of time (see Fig. 5), whereas the remaining part of the ^{1}H NMR spectrum was averaged. Moreover, for the C-1 and C-3 imide carbon signals, a reminiscence of the conformational freeze-out was observed. Interestingly, the chemical shifts of the split imide signals on both ^{1}H and ^{13}C NMR spectra were equal to those observed in regular room temperature spectra.

The linear negative temperature dependence of the imide-NH chemical shifts in $CDCl_3$ ($\Delta\delta_{NH}/\Delta T$ values of −0.020 and −0.019 ppm, respectively, for **A** and **B**) suggests the formation of intermolecular hydrogen bonds between the respective invertomers, most probably similar to those observed in the solid state. Thus, it would be tempting to ascribe the aforementioned spectroscopic features to the head-to-head molecular self-assembly of **A** and **B** to form a cyclic dimer **AB** at low temperatures. This interpretation would lead to the assumptions that (1) the temporarily arrested dynamics of the imide fragment of the molecule is not observed in hydrogen-bonding competing solvents; (2) the formation of the dimeric form **AB** (not **AA**, **BB**) takes place exclusively at low temperatures; (3) the energy of the hydrogen bonding is higher than the interconversion barriers of **A** to **B** at room temperature; (4) the equilibrium between the hydrogen-bonded and the non-hydrogen-bonded species is the cause of averaging of the NMR res-

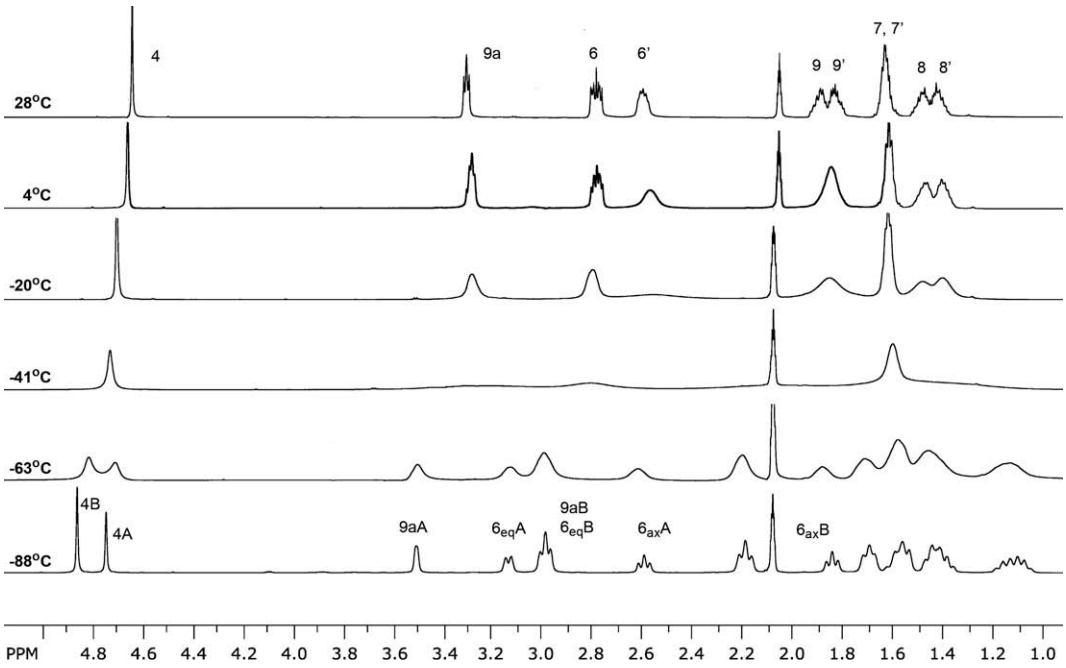

Figure 4. Aliphatic region of the low-temperature ^{1}H NMR (500 MHz, acetone-d_6) spectra of (4*R*,9a*R*)-**6**.

Table 5
Selected ^{1}H and ^{13}C NMR shifts (500 MHz, acetone-d_6, −88 °C) of (4*R*,9a*R*)-**6** (ppm)

Position	Conformer **A**		Conformer **B**	
	δ_H	δ_C	δ_H	δ_C
2	10.99		11.15	
4	4.79	69	4.91	68.1
6	3.18 (*eq*)	50.6	3.02 (*eq*)	50.2
	2.63 (*ax*)		1.88 (*ax*)	
7	1.73 (*eq*)	25.4	1.60 (*eq*)	24.6
	1.65 (*ax*)		1.49 (*ax*)	
8	1.64 (*eq*)	20.6	1.77 (*eq*)	23.6
	1.20 (*ax*)		1.14 (*ax*)	
9	2.22 (*eq*)	24	2.25 (*eq*)	28
	1.50 (*ax*)		1.44 (*ax*)	
9a	3.55	53.7	3.01	56.5

onances in the imide moiety shortly after decooling to room temperature. Indeed, the temperature spectra recorded in CD_3OD did not divulge any division of the imide C-1 and C-3 resonances after warming. Moreover, the self-association of (4*R*,9a*R*)-**6** appears to be distinct at room temperature, as judged from a positive concentration dependence of the averaged chemical shift of the imide-NH resonance. Nevertheless, the complete evaluation of the proposed explanation requires further investigations in detail, which will be presented in due course.

3. Conclusions

4-Phenyl-perhydropyrido[1,2-*a*]pyrazine-1,3-diones (4*R*,9a*S*)-**4**, (4*S*,9a*R*)-**4,** (4*S*,9a*S*)-**6**, and (4*R*,9a*R*)-**6** having potential biological activity can be prepared in enantiopure forms using a simple and efficient synthetic pathway. The results of the ^{1}H NMR experiments and chiral HPLC analyses show that no epimerization at the C-9a stereocenter of the reaction products occurs during exposure to bases. The partial epimerization of the relatively acidic H-4 proton can be avoided when a strong base is used at room temperature for the rapid cyclocondensation reaction of **3** to **4**.

Elucidation of structure using NMR and XRD shows very pronounced differences between the diastereomeric (4*R*,9a*R*)-**6**/(4*S*,9a*R*)-**4** pair. Analysis of the dynamic processes influencing the ^{1}H NMR spectra of (4*R*,9a*R*)-**6** shows the coexistence of two

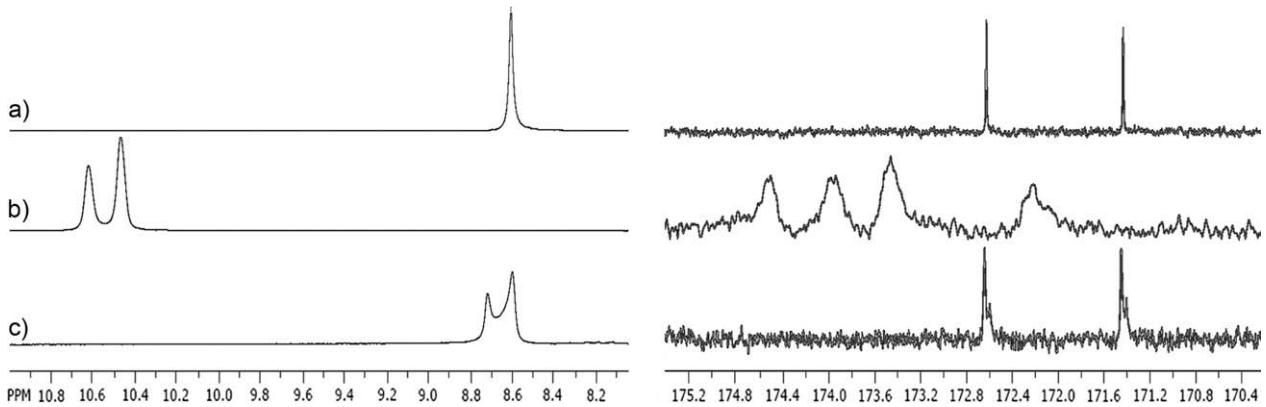

Figure 5. Signals of NH proton (left) and C-1, C-3 carbons (right) of the imide moiety of (4*R*,9a*R*)-**6** at (a) room temperature, (b) −65 °C, and (c) after warming to room temperature (500 MHz, $CDCl_3$).

invertomers in solution. It is probable that self-aggregation of the conformers restrains the dynamic processes in the imide parts of the molecules. The NMR-derived model of the respective invertomers is in agreement with the XRD data, which shows the unusual coexistence of both species in the solid state. On the contrary, due to steric reasons, (4*S*,9a*R*)-**4** exists in a single conformation and tends to be especially rigid in solution.

4. Experimental

4.1. General methods

Melting points were determined on an Electrothermal 9100 apparatus with open capillary tubes and are uncorrected. The IR spectra were obtained on a Shimadzu FTIR-8300 spectrometer. The ^{1}H, ^{13}C, NOE, and 2D-NMR spectra were recorded on a Varian Unity Plus–500 MHz spectrometer. In some cases, the ^{1}H NMR spectra were obtained on a Varian NMR–700 MHz apparatus. Chemical shifts (δ) are expressed in parts per million relative to tetramethylsilane used as the internal reference. Coupling constants (J) are in hertz (Hz). GC/MS analyses were conducted on a Hewlett Packard HP-5890 apparatus with an MSD 5972 spectrometer. ESI-HRMS analyses were done on a Mariner (PE Biosystems) instrument. EI-HRMS and EI-LRMS spectra were obtained on AMD 604 (AMD Intectra GmbH) spectrometer. Specific rotations were measured with a PolAA 32 (Optical Activity Ltd) Polarimeter at 20 °C. Thin-layer chromatography was run on Merck Silica Gel-60 F_{254} plates. The compounds were visualized by UV light (254 nm) or iodine. Flash column chromatography was carried out on Merck Silica gel 60 (230–400 mesh ASTM). HPLC analyses were carried out for compound **3** on a Chiralpak AD column, 10 μm, 250 × 4.6 mm, with mobile phase: *n*-hexane/ethanol 95:5, flow rate 1.0 mL/min; and for compound **4** on Chiralcel OD column, 10 μm, 250 × 4.6 mm, with mobile phase: 2-propanol, flow rate: 0.5 mL/min (both columns from Daicel Chiral Technologies Europe, Cedex, France). The sample concentration was approximately 0.2 mg/mL, injection: 10 μL, temperature: 25 °C, detection 220 nm. All reagents were purchased from commercial sources and were used as received. (*R*)-(+)- and (*S*)-(−)-2-piperidinecarboxylic acids,[10] (*R*)-(−)- and (*S*)-(+)-2-(4-toluenesulfonyloxy)-phenylacetic acid methyl esters[5,7] were obtained in high enantiomeric purities (ee ⩾ 99%) by known procedures, and their physicochemical constants were in agreement with literature data.

4.2. Preparation of (*S*)-(−)- and (*R*)-(+)-2-piperidinecarboxamides 1

To a stirred, cooled (−20 °C) solution of the amino acid (14 g, 0.108 mol) in anhydrous methanol (200 mL, 4.938 mol), thionyl chloride (7.9 mL, 0.108 mol) was added dropwise, while maintaining the temperature below 0 °C. The mixture was then allowed to reach room temperature and heated at reflux until sulfur dioxide ceased to evolve (2 h). The solution was then concentrated under reduced pressure, and traces of unreacted thionyl chloride were coevaporated with dry toluene (2 × 20 mL). The resulting white solid was suspended in ethyl acetate (100 mL), and triethylamine (15.1 mL, 0.108 mol) was added in one portion. The suspension was stirred at room temperature overnight. The solids were filtered off and washed with ethyl acetate. The combined filtrates were dried with anhydrous sodium sulfate, filtered, and concentrated under reduced pressure. The resulting pale yellow oil was dissolved in saturated methanolic ammonia (100 mL), and the resulting mixture was allowed to stand at room temperature for two days. The solution was then concentrated under reduced pressure to yield a pale yellow solid, which gave the title compound after recrystallization from toluene.

4.2.1. (*S*)-(−)-2-Piperidinecarboxamide (*S*)-1

Yield: 71%; white solid; mp 163–165 °C {lit.[11] mp 162–163 °C}; $[\alpha]_D = -33.4$ (*c* 3.2, EtOH); {lit.[11] $[\alpha]_D = -32.4$ (*c* 3.2, H_2O)}; IR (KBr): 1319, 1408, 1636, 2831, 2939, 3194, 3306, 3387; ^{1}H NMR ($CDCl_3$, 500 MHz): δ 1.39–1.50 (m, 3H), 1.56–1.61 (m, 1H), 1.69 (br s, 1H), 1.80–1.84 (m, 1H), 1.96–2.00 (m, 1H), 2.66–2.71 (m, 1H), 3.02–3.06 (m, 1H), 3.20–3.23 (m, 1H), 5.41 (br s, 1H), 6.67 (br s, 1H); ^{13}C NMR ($CDCl_3$, 125 MHz): δ 24.1, 26.0, 30.0, 45.8, 60.3, 177.2

4.2.2. (*R*)-(+)-2-Piperidinecarboxamide (*R*)-1

Yield: 83%; white solid; mp = 164–166 °C {lit.[12] mp 114–115 °C}; $[\alpha]_D = +33.5$ (*c* 2.3, EtOH) {lit.[11] $[\alpha]_D = +31.6$ (*c* 2.3, EtOH)}.

4.3. General procedure for the preparation of (2-carbamoylpiperidinyl)-α-phenylacetic acid methyl esters 3

A mixture of **1** (0.32 g, 2.5 mmol), **2** (0.80 g, 2.5 mmol), and pyridine (0.22 mL, 2.8 mmol) in acetonitrile (15 mL) was stirred at reflux for 1 h. The volatiles were then evaporated under reduced pressure, and the pale yellow semisolid residue was partitioned between ethyl acetate (40 mL) and water (15 mL). The mixture was transferred to a separatory funnel, and the layers were separated. The aqueous layer was extracted with ethyl acetate (15 mL). The combined organic extracts were washed with water (10 mL) and brine (10 mL), dried with anhydrous magnesium sulfate, filtered, and concentrated under reduced pressure. The crude product was purified by column chromatography (hexane/ethyl acetate 2:1, v/v; then ethyl acetate) to furnish the desired products. Analytical samples of the pure diastereomers were prepared by recrystallization from *n*-heptane/diethyl ether (1:1, v/v).

4.3.1. (2*S*,α*R*)-α-(2-Carbamoylpiperidinyl)-α-phenylacetic acid methyl ester (2*S*,α*R*)-3

White solid; mp 111–112 °C; $[\alpha]_D = -125.0$ (*c* 1, $CHCl_3$); IR (KBr): 694, 733, 1686, 1744, 2858, 2932, 3221, 3263, 3441; TLC (hexane/ethyl acetate 1:2): $R_f = 0.34$; ^{1}H NMR ($CDCl_3$, 500 MHz): δ 1.25–1.33 (m, 1H, H-5_{ax}), 1.36–1.43 (m, 1H, H-4_{ax}), 1.43–1.50 (m, 1H, H-5_{eq}), 1.52–1.61 (m, 1H, H-4_{eq}), 1.78–1.86 (m, 8 lines, $^{2}J_{3ax\text{-}3eq} = 14.0$, $^{3}J_{3ax\text{-}4ax} = 9.5$, $^{3}J_{3ax\text{-}4eq} = 5.0$, $^{3}J_{3ax\text{-}2eq} = 5.0$, 1H, H-$3_{ax}$), 1.92–1.99 (m, 1H, H-$3_{eq}$), 2.20–2.26 (m, 8 lines, $^{2}J_{6ax\text{-}6eq} = 13.0$, $^{3}J_{6ax\text{-}5ax} = 6.5$, $^{3}J_{6ax\text{-}5eq} = 3.5$, 1H, H-$6_{ax}$), 2.82–2.91 (m, 7 lines, $^{2}J_{6eq\text{-}6ax} = 13.0$, $^{3}J_{6eq\text{-}5ax} = 9.0$, $^{3}J_{6eq\text{-}5eq} = 3.0$, 1H, H-$6_{eq}$), 3.17 (pt, $^{3}J_{2\text{-}3ax,3eq} = 5.0$, 1H, H-2), 3.69 (s, 3H, OCH_3), 4.74 (s, 1H, H-α), 6.04 (bs, 1H, NH), 7.25 (bs, 1H, NH'), 7.32–7.39 (m, 5H, H-2′, H-3′, H-4′, H-5′, H-6′); ^{13}C NMR ($CDCl_3$, 125 MHz): δ 21.9 (C-4), 22.2 (C-5), 24.3 (C-3), 45.3 (C-6), 52.2 (C-OCH_3), 61.8 (C-2), 68.6 (C-α), 128.5 (C-4′), 128.6 (C-2′, C-6′), 129.4 (C-3′, C-5′), 134.1 (C-1′), 172.7 ($CONH_2$), 176.0 (COOMe); HPLC: retention time: 21.5 min; GC/LRMS: retention time: 35.3 min, LRMS (EI, 70 eV) *m/z* (relative intensity): 232 ($[M-CONH_2]^+$, 100), 217 (7), 172 (13), 149 (19), 121 (53), 91 (13), 84 (10), 77 (9); HRMS (ESI) calcd for $C_{15}H_{20}N_2O_3Na$: 299.1366 $[M+Na]^+$; found 299.1364.

4.3.2. (2*R*,α*S*)-α-(2-Carbamoylpiperidinyl)-α-phenylacetic acid methyl ester (2*R*,α*S*)-3

White solid; mp 110–112 °C; $[\alpha]_D = +124.6$ (*c* 1, $CHCl_3$); HPLC: retention time: 30.4 min; HRMS (ESI) calcd for $C_{15}H_{20}N_2O_3Na$: 299.1366 $[M+Na]^+$; found 299.1376.

4.3.3. (2*S*,α*S*)-α-(2-Carbamoylpiperidinyl)-α-phenylacetic acid methyl ester (2*S*,α*S*)-5

White solid; mp 92–93 °C; $[\alpha]_D = +3.0$ (*c* 1, $CHCl_3$); IR (KBr): 698, 748, 1682, 1736, 2851, 2932, 2931, 3209, 3321, 3460; TLC (hexane/ethyl acetate 1:2): $R_f = 0.28$; ^{1}H NMR ($CDCl_3$, 500 MHz): δ 1.30–1.35 (m, 1H, H-5_{ax}), 1.50–1.72 (m, 4H, H-3_{ax}, H-4_{ax}, H-4_{eq}, H-5_{eq}),

1.83–1.90 (m, 1H, H-3$_{eq}$), 2.74–2.80 (m, 8 lines, $^2J_{6ax\text{-}6eq}$ = 13.7, $^3J_{6ax\text{-}5ax}$ = 5.6, $^3J_{6ax\text{-}5eq}$ = 3.8, 1H, H-6$_{ax}$), 2.91–2.98 (m, 7 lines, $^2J_{6eq\text{-}6ax}$ = 13.7, $^3J_{6eq\text{-}5ax}$ = 9.5, $^3J_{6eq\text{-}5eq}$ = 3.2, 1H, H-6$_{eq}$), 3.19 (pt, $^3J_{2\text{-}3ax,3eq}$ = 4.5, 1H, H-2), 3.70 (s, 3H, OCH_3), 4.77 (s, 1H, H-α), 6.03 (bs, 1H, NH), 7.20 (bs, 1H, NH'), 7.31–7.37 (m, 3H, H-3′, H-4′, H-5′), 7.41 (dt, ^3J = 9.0, ^4J = 2.0, 2H, H-2′, H-6′); ^{13}C NMR ($CDCl_3$, 125 MHz): δ 21.6 (C-5), 22.0 (C-4), 23.8 (C-3), 46.5 (C-6), 52.0 (C-OCH_3), 59.9 (C-2), 67.9 (C-α), 128.4 (C-2′, C-6′), 128.8 (C-3′, C-5′), 128.8 (C-4′), 136.0 (C-1′), 172.2 ($CONH_2$), 176.1 (COOMe); HPLC: retention time: 24.9 min); GC/MS: retention time: 35.6 min, LRMS (EI, 70 eV) *m/z* (rel. intensity): 232 ([M-$CONH_2$]$^+$, 100), 217 (10), 172 (23), 149 (29), 121 (56), 91 (17), 84 (18), 77 (12); HRMS (ESI) calcd for $C_{15}H_{20}N_2O_3Na$: 299.1366 [M+Na]$^+$; found 299.1365.

4.3.4. (2*R*,α*R*)-α-(2-Carbamoylpiperidinyl)-α-phenylacetic acid methyl ester (2*R*,α*R*)-5

White solid; mp 93–94 °C; $[\alpha]_D$ = −3.7 (*c* 1, $CHCl_3$); HPLC: retention time: 28.1 min; HRMS (ESI) calcd for $C_{15}H_{20}N_2O_3Na$: 299.1366 [M+Na]$^+$; found 299.1361.

4.4. General procedure for the preparation of 4-phenyl-perhydropyrido[1,2-*a*]pyrazine-1,3-diones 4

To the stirred solution of **3** (0.40 g, 1.6 mmol) in absolute ethanol (10 mL), sodium hydroxide (65 mg, 1.6 mmol) pellet was added at room temperature. After complete dissolution of the hydroxide, the mixture was stirred for an additional 5 min and quenched with saturated aqueous ammonium chloride (30 mL). The resulting cloudy solution was extracted with ethyl acetate (2 × 30 mL). The combined organic extracts were sequentially washed with water (10 mL) and brine (10 mL), dried with magnesium sulfate, filtered, and concentrated under reduced pressure. Analytically pure isomers were obtained by a single recrystallization from minimal amount of absolute ethanol.

4.4.1. (4*R*,9a*S*)-4-Phenyl-perhydropyrido[1,2-*a*]pyrazine-1,3-dione (4*R*,9a*S*)-4

Colorless crystals; mp 188–189 °C (dec.); $[\alpha]_D$ = −137.4 (*c* 1, $CHCl_3$); IR (KBr): 698, 760, 1231, 1693, 1732, 2851, 2924, 3213; TLC (hexane/ethyl acetate 5:3): R_f = 0.33; ^{1}H NMR ($CDCl_3$, 700 MHz): δ 1.34 (4t, $^2J = {}^3J_{ax\text{-}ax}$ = 13.3, $^3J_{ax\text{-}eq}$ = 3.5, 1H, H-8$_{ax}$), 1.42 (4t, $^2J = {}^3J_{ax\text{-}ax}$ = 12.6, $^3J_{ax\text{-}eq}$ = 3.5, 1H, H-7$_{ax}$), 1.55 (2quin, ^2J = 15.6, 1H, H-7$_{eq}$), 1.59–1.66 (m, 1H, H-9$_{ax}$), 1.84 (td, $^2J = {}^3J_{ax\text{-}ax}$ = 11.9, $^3J_{ax\text{-}eq}$ = 2.8, 1H, H-6$_{ax}$), 1.86–1.90 (m, ^2J = 12.6, 1H, H-8$_{eq}$), 2.42 (2quin, 1H, H-9$_{eq}$), 2.75 (dt, ^2J = 11.2, $^3J_{ax\text{-}eq,eq\text{-}eq}$ = 2.1, 1H, H-6$_{eq}$), 2.99 (dd, $^3J_{9a\text{-}9ax}$ = 11.2, $^3J_{9a\text{-}9eq}$ = 2.8, 1H, H-9a), 3.93 (s, 1H, H-4), 7.33–7.40 (m, 5H, H-2′, H-3′, H-4′, H-5′, H-6′), 8.18 (br s, 1H, NH, D_2O washable); ^{13}C NMR ($CDCl_3$, 125 MHz): 23.5 (C-8), 25.0 (C-7), 27.1 (C-9), 53.3 (C-6), 63.2 (C-9a), 72.1 (C-4), 128.5 (C-2′, C-6′), 128.6 (C-4′), 129.2 (C-3′,C-5′), 136.2 (C-1′), 170.9 (C-3), 171.5 (C-1); HPLC: retention time: 17.5 min; LRMS (EI, 70 eV) *m/z* (rel. intensity): 244 ([M]$^+$, 21), 172 (100), 91 (12), 84 (40); HRMS (EI) calcd for $C_{14}H_{16}N_2O_2$: 244.1212; found 244.1223.

4.4.2. (4*S*,9a*R*)-4-Phenyl-perhydropyrido[1,2-*a*]pyrazine-1,3-dione (4*S*,9a*R*)-4

Colorless crystals; mp 187–189 °C (dec.); $[\alpha]_D$ = +138.3 (*c* 1, $CHCl_3$); HPLC: retention time: 19.6 min; LRMS (EI, 70 eV) *m/z* (rel. intensity): 244 ([M]$^+$, 27), 172 (100), 91 (4), 84 (36); HRMS (EI) calcd for $C_{14}H_{16}N_2O_2$: 244.1212; found 244.1218.

4.4.3. (4*S*,9a*S*)-4-Phenyl-perhydropyrido[1,2-*a*]pyrazine-1,3-dione (4*S*,9a*S*)-6

Colorless crystals, mp 150–151 °C (dec.);$[\alpha]_D$ = −97.1 (*c* 1, $CHCl_3$); IR (KBr): 694, 733, 1265, 1238, 1312, 1693, 1736 2816, 2924, 2943, 3086, 3198, 3221; TLC (hexane/ethyl acetate 5:3): R_f = 0.41; ^{1}H NMR ($CDCl_3$, 700 MHz): δ 1.43–1.52 (m, 2H, H′-8, H-8), 1.64–1.70 (m, 2H, H′-7, H-7), 1.79–1.86 (m, 1H, H′-9), 2.00–2.06 (m, 1H, H-9), 2.64–2.69 (m, 1H, H′-6), 2.71–2.76 (m, 1H, H-6), 3.41 (pt, 1H, H-9a), 4.61 (s, 1H, H-4), 7.33–7.40 (m, 5H, H-2′, H-3′, H-4′, H-5′, H-6′), 8.13 (br s, 1H, NH, D_2O washable); ^{13}C NMR ($CDCl_3$, 125 MHz): δ 21.6 (C-8), 24.9 (C-7), 25.3 (C-9), 50.8 (C-6), 55.1 (C-9a), 69.2 (C-4), 127.9 (C-2′, C-6′), 128.5 (C-4′), 128.8 (C-3′, C-5′), 132.7 (C-1′), 171.6 (C-3), 172.7 (C-1); HPLC: retention time: 11.2 min; LRMS (EI, 70 eV) *m/z* (rel. intensity): 244 ([M]$^+$,32), 172 (100), 91 (8), 84 (81); HRMS (EI) calcd for $C_{14}H_{16}N_2O_2$: 244.1212; found 244.1217.

4.4.4. (4*R*,9a*R*)-4-Phenyl-perhydropyrido[1,2-*a*]pyrazine-1,3-dione (4*R*,9a*R*)-6

Colorless crystals, mp 150–151 °C (dec.); $[\alpha]_D$ = +96.6 (*c* 1, $CHCl_3$); HPLC: retention time: 10.1 min; LRMS (EI, 70 eV) *m/z* (rel. intensity): 244 ([M]$^+$,30), 172 (100), 91 (6), 84 (48); HRMS (EI) calcd for $C_{14}H_{16}N_2O_2$: 244.1212; found 244.1215.

4.5. X-ray crystallographic determination of (4*R*,9a*R*)-6

The crystalline and molecular structures were determined by X-ray diffraction. Crystals suitable for X-ray analysis were grown from EtOH solution by slow evaporation. The data were collected on an Oxford Diffraction KM4CCD diffractometer,[13] using graphite-monochromated Mo Kα radiation, at 293 K. The unit-cell parameters were determined by the least-squares treatment of setting angles of highest-intensity reflections chosen from the whole experiment. Intensity data were corrected for the Lorentz and polarization effects.[14] The structure was solved by the direct method using the SHELXS-97 program[15] and refined by the full-matrix least-squares method with the SHELXL97 program.[16] The function $\Sigma w(|F_o|^2 - |F_c|^2)^2$ was minimized with $w^{-1} = [\sigma^2(F_o)^2 + (0.0478P)^2 + 0.0394P]$ for (4*R*,9a*R*)-**6**, where $P = (F_o^2 + 2F_c^2)/3$. An empirical extinction correction was also applied for (4*R*,9a*R*)-**6**, according to the formula $F'_c = kF_c[1 + (0.001\chi F_c^2\lambda^3/\sin 2\theta)]^{-1/4}$,[16] and the extinction coefficient χ was equal to 0.040(3). All non-H atoms were refined anisotropically; positions of hydrogen atoms were generated geometrically and refined as a riding model. Thermal parameters of all hydrogen atoms were calculated as 1.2 times U_{eq} of the respective carrier carbon atom. The figures were drawn using the MERCURY program.[17]

The deposition number CCDC 725959 for (4*R*,9a*R*)-**6** contains the supplementary crystallographic data from this study. These data can be obtained free of charge through www.ccdc.cam.ac.uk/data_request/cif, or by emailing data_request@ccdc.cam.ac.uk, or by contacting The Cambridge Crystallographic Data Centre, 12, Union Road, Cambridge CB2 1EZ, UK; fax: +44 1223 336033.

4.5.1. Crystal data for (4*R*,9a*R*)-6

$C_{14}H_{16}N_2O_2$, M = 244.29, D_{calcd} = 1.290 g/cm^3, monoclinic, $P2_1$, a = 11.4703(3) Å, b = 8.5759(2) Å, c = 13.2163(4) Å, β = 104.700(3)°, V = 1257.51(6) Å^3, Z = 4, F(0 0 0) = 520, μ = 0.088 mm^{-1}. The reflections collected numbered 28615, of which 4728 were unique [R(int) = 0.0203]; 4088 reflections $I > 2\sigma(I)$, R_1 = 0.0274 and wR_2 = 0.0711 for 4088 [$I > 2\sigma(I)$] and R_1 = 0.0351 and wR_2 = 0.0785 for all (4728) intensity data. Goodness of fit = 1.087; residual electron densities in the final Fourier map were 0.124 and −0.132 e Å^{-3}.

References

1. (a) Kamiński, K.; Obniska, J. *Bioorg. Med. Chem.* **2008**, *16*, 4921–4931; (b) Abdel-Hafez, A. A.-M. *Arch. Pharm. Res.* **2004**, *27*, 495–501; (c) Boerenstein, M. R.; Doukas, P. H. US Patent 4 925 841, 1990.; (d) Malawska, B. *Curr. Top. Med. Chem.* **2005**, *5*, 69–85.

2. (a) Luzzio, F. A.; Mayorov, A. V.; Ng, S. S. W.; Kruger, E. A.; Figg, W. D. *J. Med. Chem.* **2003**, *46*, 3793–3799; (b) Lepper, E. R.; Ng, S. S. W.; Gutschow, M.; Weiss, M.; Hecker, T. K.; Luzzio, F. A.; Eger, K.; Figg, W. D. *J. Med. Chem.* **2004**, *47*, 2219–2227; (c) Dredge, K.; Marriott, J. B.; Macdonald, C. D.; Man, H. W.; Chen, R.; Muller, G. W.; Stirling, D.; Dalgleish, A. G. *Br. J. Cancer* **2002**, *87*, 1166–1172.
3. (a) Caliendo, G.; Santagada, V.; Perissutti, E.; Fiorino, F. *Curr. Med. Chem.* **2005**, *12*, 1721–1753; (b) Lopez-Rodriguez, M. L. et al *J. Med. Chem.* **2005**, *48*, 2548–2558; (c) López-Rodríguez, M. L.; Ayala, D.; Benhamú, B.; Morcillo, M. J.; Viso, A. *Curr. Med. Chem.* **2002**, *9*, 443–469; (d) Herold, F.; Król, M.; Kleps, J.; Nowak, G. *Eur. J. Med. Chem.* **2006**, *41*, 125–134; (e) Herold, F.; Chodkowski, A.; Izbicki, Ł.; Król, M.; Kleps, J.; Turło, J.; Nowak, G.; Stachowicz, K.; Dybała, M.; Siwek, A. *Eur. J. Med. Chem.* doi: 10.1016/j.ejmech.2008.09.021.
4. (a) Dinsmore, C. J.; Beshore, D. C. *Tetrahedron* **2002**, *58*, 3297–3312; (b) Fytas, C.; Zoidis, G.; Fytas, G. *Tetrahedron* **2008**, *64*, 6749–6754; (c) Tanabe, K.; Ikegami, Y.; Ishida, R.; Andoh, T. *Cancer Res.* **1991**, *51*, 4903–4908; (d) Cai, J. C.; Shu, H. L.; Tang, C. F.; Komatsu, T.; Matsuno, T.; Narita, T.; Yaguchi, S.; Koide, Y.; Takase, M. *Chem. Pharm. Bull.* **1989**, *37*, 2976–2983; (e) Suaifan, G. A. R. Y.; Mahon, M. F.; Arafat, T.; Threadgill, M. D. *Tetrahedron* **2006**, *62*, 11245–11266; (f) Deveau, A. M.; Costa, N. E.; Joshi, E. M.; Macdonald, T. *Bioorg. Med. Chem. Lett.* **2008**, *18*, 3522–3525; (g) Martins, M. B.; Carvalho, I. *Tetrahedron* **2007**, *63*, 9923–9932; (h) Perotta, E.; Altamura, M.; Barani, T.; Bindi, S.; Giannotti, D.; Harmat, N. J. S.; Nannicini, R.; Maggi, C. A. *J. Comb. Chem.* **2001**, *3*, 453–460.
5. Herold, F.; Dawidowski, M.; Wolska, I.; Chodkowski, A.; Kleps, J.; Turło, J.; Zimniak, A. *Tetrahedron: Asymmetry* **2007**, *18*, 2091–2098.
6. Belostotskii, A. M.; Markevich, E. *J. Org. Chem.* **2003**, *68*, 3055–3063. and references cited therein.
7. (a) Curotto, G.; Donati, D.; Finiza, G.; Ursini, A. *Tetrahedron: Asymmetry* **1995**, *6*, 849–852; (b) Curotto, G.; Donati, D.; Finiza, G.; Ursini, A. *Tetrahedron* **1997**, *53*, 7347–7364.
8. (a) Karplus, M. *J. Chem. Phys.* **1959**, *30*, 11–15; (b) Karplus, M. *J. Am. Chem. Soc.* **1963**, *85*, 2870–2871.
9. Günther, H. *NMR Spectroscopy. An Introduction*; John Wiley & Sons: New York, 1980.
10. Ho, B.; Venkatarangan, P.; Cruse, S.; Hinko, C.; Andersen, P.; Crider, A.; Adloo, A.; Roane, D.; Stables, J. *Eur. J. Med. Chem.* **1998**, *33*, 23.
11. Perumattam, J.; Shearer, B. G.; Confer, W. L.; Mathew, R. M. *Tetrahedron Lett.* **1991**, *32*, 7183.
12. Somlai, C.; Balaspiri, L. *Acta Chim. Hung.* **1992**, *129*, 871–877.
13. Oxford Diffraction Poland, CrysAlisCCD, CCD data collection GUI, version 1.171.32.5, 2007.
14. Oxford Diffraction Poland, CrysAlisRED, CCD data reduction GUI, version 1.171.32.5, 2007.
15. Sheldrick, G. M. *Acta Crystallogr., Sect. A* **1990**, *46*, 467–473.
16. Sheldrick, G. M. SHELXL *97*: *Program for the Refinement of Crystal Structures*, University of Göttingen: Germany, 1997.
17. Mercury visualization and analysis of crystal structures: Macrae, C. F.; Edgington, P. R.; McCabe, P.; Pidcock, E.; Shields, G. P.; Taylor, R.; Towler, M.; van de Streek, J. *J. Appl. Cryst.* **2006**, *39*, 453–457.